Research Programs

Density Distribution in Powder Metal Compacts: Prediction & Control

Mr. Jayant Khambekar
Prof. Mark W. Richman

In this project we consider single punch compaction of powder metals in hollow cylindrical geometries. In the first phase of the project, we determine how non-uniform initial powder fill affects the evolution of the density distributions during compaction. Special attention is paid to the density distribution in the resulting green compact. In the second phase, we determine an appropriate model for the dependence of coefficient of friction and radial-to-axial pressure ratio on density and pressure during compaction, and employ the model to predict the evolution of the pressure and density variations as compaction proceeds. In the third phase, we develop a remarkably simple model to predict how the required ejection force varies with punch displacement after the compaction pressure is removed. Brief descriptions of the three phases as well as typical results from each and are given below.

In studying the effects of non-uniform initial density distribution, we confront the unavoidable fact that due to uneven fill, powder densities vary with initial location in the die. . The extent of uneven fill in the axial direction, for example, is measured by the percent top-to-bottom density increase, denoted by Δ_z. The subsequent compaction process is modeled using equations of equilibrium in the axial and radial directions, a constitutive relation that relates the axial pressure to the radial pressure at any point in the specimen, and a plausible equation of state that relates local density to the local pressure. Coulomb friction is assumed to act at the interfaces between the specimen and both the die wall and core rod. In this manner, we determine the axial and radial variations of the final density, the axial, radial and tangential pressures, and the shear stress. Of special interest are the inverse problems, in which we find the required non-uniform initial density distribution that, in principle, will yield no variation in the final green density.

Typical results obtained in this phase are shown in Figure 1, in which we predict the evolution of the top-to-bottom density decrease δ_z during the compaction for three different cases: Δ_z=10%, 0%, -10%. The stage of compaction is measured by the ratio of the current height H of the cylinder to its initial height L. The results apply when the ratio of the inside radius R_i to the outside radius R_o is equal to .5, L/R_o=8.88, the coefficients of friction μ_i and μ_o at the core rod and die wall are both equal to .2, the average density η in

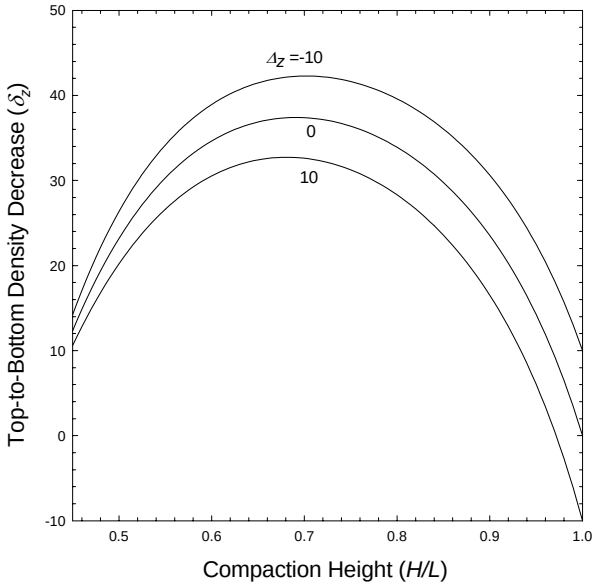

Figure 1: Variation of δ_z with H/L for different cases Δ_z =10, Δ_z =0 and Δ_z =-10 and for parameter values η=.41, α=.5, L/R_o=8.88, μ_i=μ_o=.2 and R_i/R_o=.5.

the initial fill normalized by the maximum theoretical density is .41, and the radial-to-axial pressure ratio α=.5. In all three cases, because the pressures are much higher at the top than at the bottom of the compact, the top-to-bottom density decrease δ_z first increases to a maximum value. However, the compressibility of the powder is inversely related to its density, and at about *H/L*=.7, regions of lower density compress more readily than the regions of higher density even at significantly lower pressures. Consequently, at this stage of the compaction and beyond, the top-to-bottom density decrease actually diminishes. When Δ_z=0%, the final value of δ_z is 12.33%; when Δ_z=10%, the final value of δ_z is 10.59%; and when Δ_z=-10%, the final value of δ_z is 14.21%. These results are interesting because they suggest that more uniform compacts could be produced from non-uniform fills that are more dense at the bottom than at the top.

In studying the influence of pressure and density on the radial-to-axial pressure ratio as well as on the coefficients of friction between the compact and the die wall and between the compact and the core rod, we develop a model that predicts the axial variations of the pressure and density at any stage of compaction. Of special interest is a powder blend which is 99.5% by weight of Distalloy AE, .5% by weight of graphite, and 1% wax Hoechst micropulver admixed as internal lubricant. Distalloy AE is a diffusion alloyed iron powder with composition 4 wt% Ni, 1.5 wt% Cu, and .5 wt% Mo. Particle sizes range from 20 to 180 μm. The apparent density of the powder is 3.04 g/cm^3, and the theoretical maximum density is 7.33g/cm^3 (so that the relative apparent density η is equal to .41). The density-dependence of the radial-to-axial pressure ratio α is based on the experimental measurements of Trassoras et.al. [1998], described by,

$$\alpha = \frac{3-b}{3+2b} \quad , \tag{1}$$

where b is a function of relative density ρ given by

$$b(\rho) = \frac{1}{2.8287}\ln\left[\frac{7.6-7.33\rho}{.2516}\right] \quad . \tag{2}$$

The pressure-dependence of the friction coefficients μ is based on the measurements of Sinka [2000] and Solimanjad et. al [2001]. A reasonable qualitative fit to their results is given by the exponential variation,

$$\mu_o = \mu_1 + (\mu_2 - \mu_1)\exp(-\phi\beta P) \quad , \tag{3}$$

where P is the pressure, β is a constant factor related to the compressibility of the loose powder, μ_2 is coefficient of friction of loose powder, μ_1 is the coefficient of friction in the most densified solid state, φ is a dimensionless parameter that reflects how rapidly μ changes with P. Typically, the coefficient of friction for the loose powder is much higher than that for the densified solid, so the variation of friction coefficient with local pressure *decays* exponentially during compaction. For the Distalloy AE of interest, β=9.75×10^{-5} in^2/lb.

As a result typical of those obtained in this phase of the project, Figure 2 shows how the percent top-to-bottom density variation evolves (from uniform) at H/L=1 at the start of compaction (to its final nonzero non-uniform value) at H/L=.5 at the end of compaction, when $\mu_i=\mu_o$ is the function $\mu(P)$ of pressure given by equations (1) and (2). Interestingly, the nonuniformity induced in the density distribution increases to a maximum (42 percent) at an intermediate height of H/L=.72 that is approximately four times the nonuniformity (10.3 percent) that is present in the final green compact. The increase in nonuniformity that occurs in the early stages of compaction is due to the fact that according to the equation of state even small top-to-bottom pressure differences give rise to fairly large density differences when the magnitudes of the pressures are low. The decrease in nonuniformity that occurs in the later stages of compaction is due to two effects. First, even if the coefficients of friction were constant throughout the compaction, the equation of state demonstrates that even large top-to-bottom pressure differences give rise to only small density differences when the magnitudes of the pressures are high. Second, the coefficient of friction, and therefore the percent top-to-bottom pressure variations diminish as compaction proceeds.

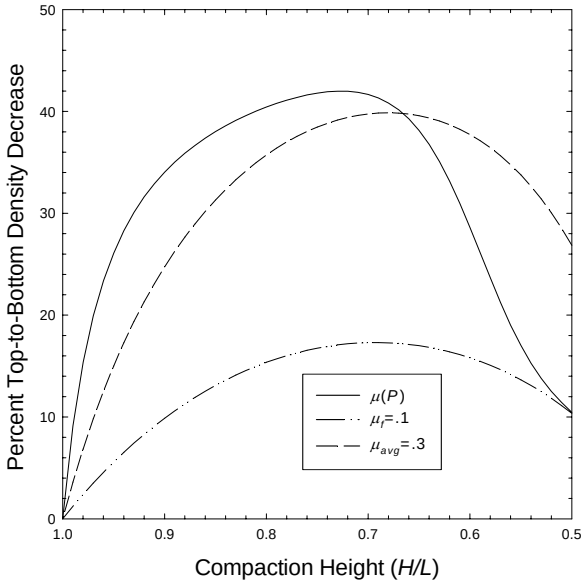

Figure 2: The variation of δ_z with H/L for three different cases of μ.. Here α .is function of pressure given by eqns. (1) and (2), $\mu(P)$ is given by equation (3) with μ_1=.1, μ_2=.9, and ϕ=1. The density distribution is initially uniform with η=.41, R_i/R_o=.5, and L/R_o=8

For the purpose of comparison, Figure 2 also shows the corresponding variations of top-to-bottom density decrease when the coefficients of friction $\mu_i=\mu_o$ are taken to be constants. In one comparison, we take $\mu_i=\mu_o$ equal to the high density value μ_1=.1, and in the other we take $\mu_i=\mu_o$ equal to an average value μ_{avg}=.302, which is appropriate to the average relative density (ρ=.615) between .41 at the start of compaction and .82 at the end. As expected, the nonuniformities predicted for minimum coefficients of friction are typically smaller than those predicted as the friction coefficients decrease to their minimum values, and the predictions approach one another as compaction concludes. The nonuniformities predicted by the $\mu_i=\mu_o=\mu_{avg}$=.302 curve, on the other hand, are smaller than those predicted by the $\mu_i=\mu_o=\mu(P)$ curve in the early stages of compaction when μ_{avg} is less than $\mu(P)$, are larger than those on the $\mu_i=\mu_o=\mu(P)$ curve in the later stages of compaction when μ_{avg} is greater than $\mu(P)$, and agree well near the instant (H/L=2/3) at which μ_{avg}. is equal $\mu(P)$.

In the final phase of the project, we develop a simple two-stage model for the relaxation and ejection of the green compact. In the first stage, we model relaxation of the compact after removal of the compaction pressure as a misfit of three cylinders, representing the core rod, the compact and the die wall. The known input is the radial pressure distribution at the conclusion of compaction, and the output is the corresponding

radial pressure distributions that prevail after the compaction pressures are removed. In the second phase, we determine the variations with punch displacement of the ejection forces required to overcome friction at the core rod and die wall. An improved model includes additions to the friction forces due to the radial expansion (i.e. the Poisson effect) that occurs during ejection, while a simple theory neglects this effect.

In Figure 3, we show the variation with punch displacement of the required ejection force when the fill height L=80 mm and the compact height H=40 mm, after compaction of the Distalloy AE described above. The elastic modulii (E_C, E_D, E_R) and the Poisson's ratios (ν_C, ν_D, ν_R) of the compact, die wall , and core rod, respectively, are given in the caption. The bold line indicates the experimental results of Gethin et.al. [1994], while the solid line (denoted by the "improved theory") indicates the result obtained using the ejection analysis developed here. For comparison, also shown as a dashed curve (denoted by the "simple theory") are the predictions made when the Poisson effect during ejection is ignored. As it must, the model predicts that while the compact is fully contained within the die (i.e. 0<D<40 mm), the ejection force remains unchanged. As an increasingly larger fraction of the compact emerges, the friction between the compact and the die decreases, and the required ejection force decreases to zero when the compact is fully removed. Most notable is the excellent agreement between the magnitudes of the measured and predicted ejection forces in this range (0<D<40 mm) of punch displacement provided that the Poisson effect during ejection is included. Moreover, even in the experiments, once the compact emerges from the die, the effects of decreasing friction dominate the ejection force, which decreases to zero when the part is fully ejected. Again, in this range of punch displacement (i.e. 40 mm<D<80 mm), agreement between the experimental results and theoretical predictions is quite good provided the Poisson effect is included.

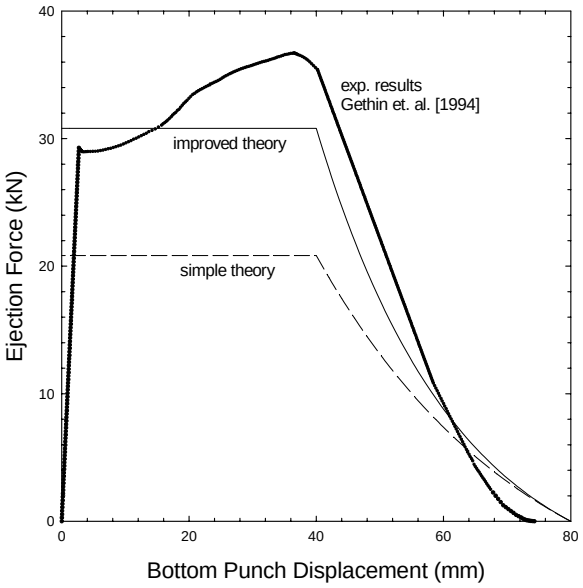

Figure 4.11: Variation of the ejection force with bottom punch for uniform initial density η=.4, μ_2=.8, μ_1=.078, φ=1, R_i/R_o=.68, H/L=.5, L/R_o=6.4, ν_C=.315, ν_D= ν_R=.3, E_C=55 GPa, E_D=E_R=200 GPa, L=80 mm, R_i=8.5 mm.

References:

Gethin, D., Ariffin, A., Tran, D., Lewis, R., (1994). Compaction and ejection of green powder compacts. Powder Metallurgy 37(1), 42-52.

Sinka, I. C., Cocks, A. C. F., Morrison, C. J., Lightfoot, A., (2000). High pressure triaxial facility for powder compaction. Powder Metallurgy 43(3), 253-261.

Solimanzad, N., Wikstrom, H., Larsson, R., (2001). A new device for measurement of friction during metal powder compaction. Proceedings of PM2TEC 2001, May 2001.

Trasorras, J. R. L., Parameswaran, R., Cocks, A. C. F., (1998). Mechanical behavior of metal powders and powder compaction modeling. ASM Handbook Volume 7, 326-342.